ISSN 0974 - 9373

Vol. 26 No. 4 (2022) **J. Int. Acad. Phys. Sci.** pp. 483-490

Electrical Simulation of Perovskite Solar Cell Using Gpvdm Software and Analysis of Power Conversion Efficiency with Variation of Perovskite Thickness

Deepak Kumar Verma
Department of Computer Science,
Dr. R.M.L. Avadh University, Ayodhya, UP, India
Email: deepak.discrete@gmail.com

Jitendra Kaushal Srivastava
Department of Electronics,
Dr. R.M.L. Avadh University, UP, India
Email: jitendra.srivastava8@gmail.com

(Received October 25, 2022, Revised November 30, 2022, Accepted December 2, 2022)

Abstract: Now-a-days, solar cell is one of the best techniques for energy harvesting. Methylammonium lead halide CH3NH3PbI3 is used as perovskite material for solar cell applications. This material is emerging as a promising new material for low-cost, high-efficiency photovoltaics. It is assumed that the perovskite material is free from defects. The solar cell simulation software GPVDM is used which works as a popular solar cell simulation tool (AMPS: Analysis of microelectronic and photonic structures). Variation in thickness of device layers yields various output characteristics of the solar cell. The simulation model solves drift-diffusion of electron and hole, carrier continuity equations in position space to describe the movement of charge within the device, poisson’s equation, and recombination of charge carriers.

1. Introduction

Perovskite material is very effectively used in photovoltaic devices like solar cells, Led, super capacitor, FET. The efficiency of the perovskite solar cell is more than 25% [1-2] , which is a very crucial factor of the perovskite solar cell industrialization. Even industrialization of the perovskite material is still challenging because of the degradation of the perovskite, we can industrialize hetrojunction of Si/Perovskite solar cells which provide better stability. We are using CH_3- NH_3PbI_3 (Perovskite)

Material as a heart of the solar cell, structure obtain[3]. Perovskite material can be electrically polarized by mechanical stress which shows the piezoelectric properties of the material. General-purpose Photovoltaic Device Model (GPVDM) is a drift–diffusion base/Shockley-Read-Hall model. This software uses a finite difference approach to solve both electron and hole drift–diffusion equations in position space to describe the movement of charges within the device. At each mesh point in position space, a set of carrier trap- ping and escape equations are solved in energy space.

We are using device structure: FTO/TiO_2/perovskite /Spiro-MeOTAD/Au for the GPVDM simulation which is useful to the optimization of the electrical and optical characteristics, in our material layer modelling we are treating defect-free material layer in the GPVDM simulation[4]. In this device structure, TiO_2 is used for electron transporting material (ETM), Spiro-MeOTAD is used for the hole transporting material (HTM) which are environment friendly, conducting and economically suitable in the device fabrication[5], perovskite is used as an active photovoltaic layer which generates charge carrier [electron and hole] contact is used for the connection of the external circuit to capture energy from the solar cell, that electrical energy we can store into a charge storing devices (super capacitor, battery, etc.)[6-12]. To studies the combined effect of the device modeling we are using GPVDM software of the electrical and optical simulation for the explanation of the PCE (power conversion efficiency) and stability of the device. The enhancement in the power conversion efficiency PCE of a $CH_3NH_3Pb_{I3}$ based solar cell by changing layers thickness.

2. Device Simulation Technique

The planer structure of the device is shown with computational structure: FTO/ETM/ $CH_3NH_3PbI_3$/ HTM/gold where TiO_2 used as an ETM (electron transporting layer) and Spiro-MeOTAD used as an HTM (hole transporting material) in the device for the carrying of electron and hole respectively. The Initial layer thickness of the nano-structured device can be chosen by the GPDVM software window. We can choose the electrical and optical parameter by GPVDM software database[13]. Study of this project is based on the changing layer thickness of the nano-structured device (PSCs) is shown in table 1. So it is found that by changing layer thickness of the device electrical parameters become changed shown in table 2.

Table 1: Layer thickness of the typical perovskite solar cell

Layer Name	Thickness(M)	Optical Matrial	Layer Type
FTO	2.5e-07	Oxide/FTO	other
TiO_2	6e-08	Oxide/TiO_2/kischkat	Other (electron transporting layer)
Perovskite	1e-07	Perovskite/std-perovskite	active
Spiro-MeOTAD	2e-08	Small maolecules/ spiroMeOTAD	Other(hole transporting layer)
Au	1e-07	Metal/Au	contact

Table 2: Simulation parameters of GPVDM software

Parameters	Value	Unit
Electron mobility	0.002	$m^2v^{-1}s^{-1}$
Hole mobility	0.002	$m^2v^{-1}s^{-1}$
Effective density of free electron states @300K	5.000×10^{26}	m^{-3}
Effective density of free hole states @300K	5.000×10^{26}	m^{-3}
n_{free} to p_{free} recombination rate constant	1.000e-15	
Electron trap density	1.0×10^{20}	$m^{-3}eV^{-1}$
Hole trap density	1.0×10^{20}	$m^{-3}eV^{-1}$
Electron tail slope	0.06	eV
Hole tail slope	0.06	eV
Free electron to trapped electron	1.0×10^{21}	m^{-2}
Trapped electron to free hole	1.0×10^{21}	m^{-2}
Trapped hole to free electron	1.0×10^{21}	m^{-2}
Free hole to trapped hole	1.0×10^{21}	m^{-2}
Number of traps	5	
Energy gap	1.6	eV
Xi	3.8	eV

3. Electrical Simulation Of Perovskite Solar Cell

The simulation parameters of the GPVDM software are shown below.

Under these parameters, I-V, current density-voltage (J-V), charge density voltage (q -V), total charge density-voltage (q_t -V) and recombi- nation-prefactor-voltage are shown in Figures 1-5, calculated at 300 K. At this temperature perovskite shows cubic structure.

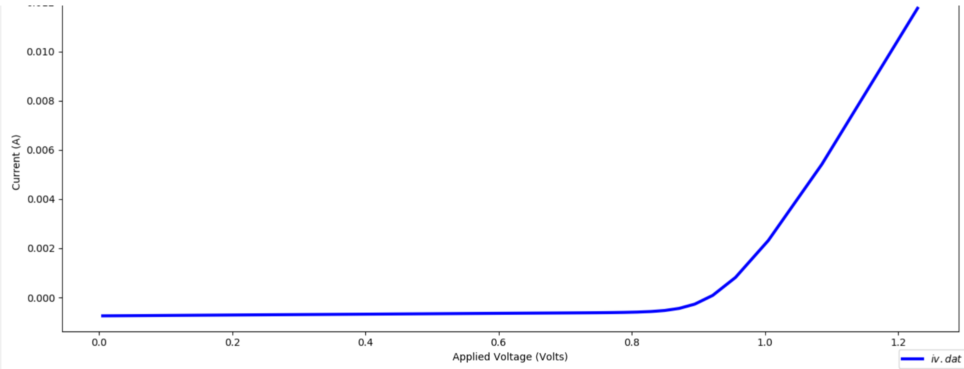

Figure 1: I-V characteristics of the perovskite solar cell at 300K

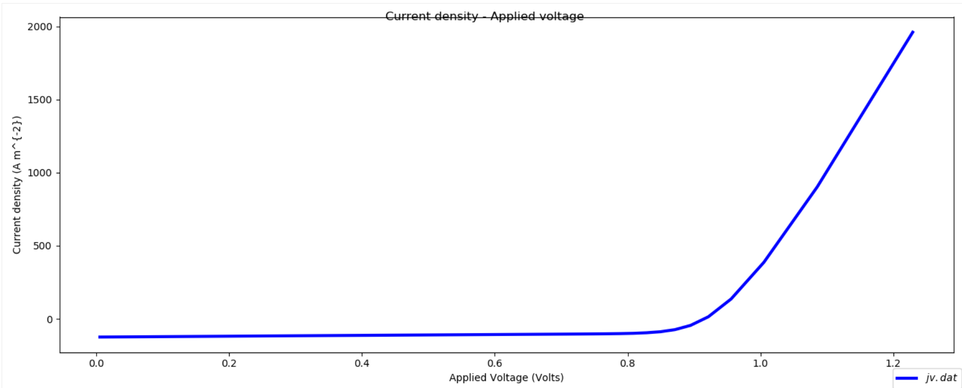

Figure 2: J-V characteristics of the perovskite solar cell at 300K

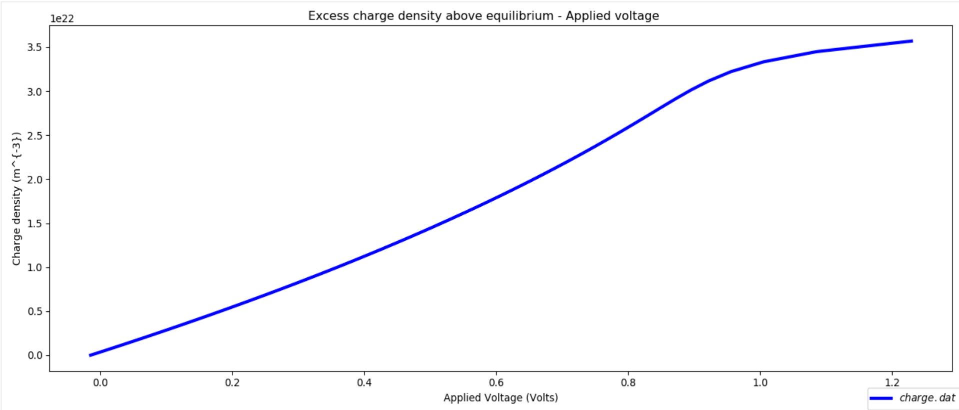

Figure 3: charge density variations with an applied voltage at 300K

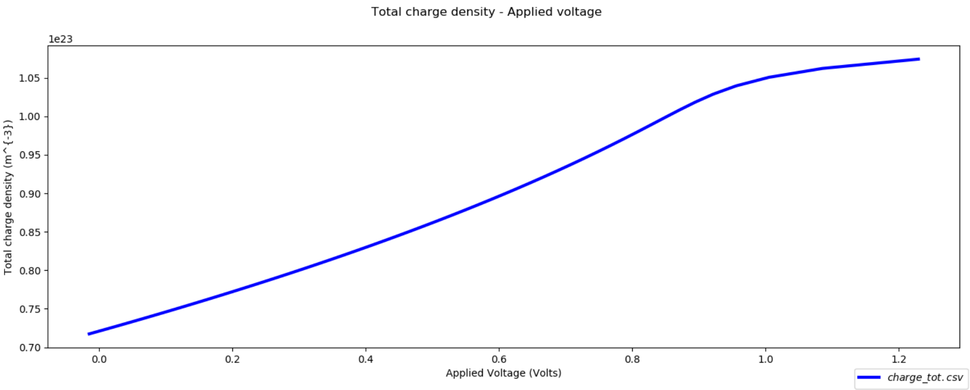

Figure 4: electron-hole contributions with an applied voltage at 300K

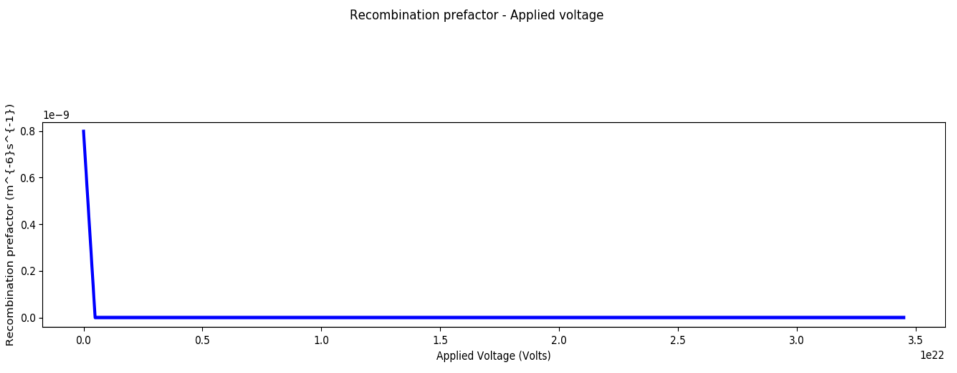

Figure 5: electron-hole pair recombination prefactor with an applied voltage across the device

The simulation information (sim info.dat.) of the perovskite solar cell simulation at various thickness has been shown in the table below. Table 3 and table 4 also show the comparative study of pervoskite solar cell.

Table 3: The electrical parameters with the variation of the layer thickness of the perovskite solar cell

Thickness (m)	V_{oc} (volts)	Current density at P_{max} (Am^{-2})	Average carrier density at P_{max} (m^{-3})	Fill factor [FF] (a.u)	Max power (watt-m^{-2})	Conversion efficiency (%)
1×10^{-7}	0.928	-1.288×10^{2}	4.981×10^{22}	0.8157	106.282	10.682
3×10^{-7}	0.9608	-1.799×10^{2}	3.6879×10^{21}	0.8418	150.9435	15.094
5×10^{-7}	0.9786	-2.170×10^{2}	5.7529×10^{20}	0.8464	185.4624	18.546
8×10^{-7}	0.9886	-2.326×10^{2}	8.7888×10^{19}	0.8490	203.087	20.308

1×10^{-6}	0.9937	-2.484×10^{2}	3.5192×10^{19}	0.8485	216.359	21.635
3×10^{-6}	0.9914	-2.548×10^{2}	2.5390×10^{19}	0.8504	221.797	22.179
4×10^{-6}	0.9866	-2.536×10^{2}	4.0749×10^{19}	0.8498	220.729	22.072
5×10^{-6}	0.9814	$-2,373\times10^{2}$	6.5108×10^{19}	0.8486	202.264	20.226

Table 4: The electrical parameter with the variation of the layer thickness of the perovskite solar cell

Thickness (m)	V_{oc} (volt)	Isc (Amp)	FF (a.u).	Maximum Power(Mpp)	Power Conversion efficiency(%)
1×10^{-7}	0.8325	69.23	79.06	45.56	4.55
2×10^{-7}	0.8420	81.91	82.16	56.67	5.6
3×10^{-7}	0.8427	75.81	83.12	53.11	5.3
4×10^{-7}	0.8407	62.83	83.37	44.04	4.40
5×10^{-7}	0.8420	58.68	83.57	41.29	4.12
6×10^{-7}	0.8420	52.81	83.60	196.33	3.72
7×10^{-7}	0.8443	48.79	83.83	34.53	3.4
8×10^{-7}	0.8433	41.05	83.96	29.07	2.9
8×10^{-7}	0.8464	41.79	83.36	29.84	2.9

We can enhance efficiency by changing the layer thickness of the perovskite layer and intermediate layer of the device. Especially in the perovskite solar cell electron and hole both works as charge carriers for energy harvesting. The dynamics of electron and hole can be analyzed by the total charge density–voltage and recombination prefactor-voltage spectra.

4. Conclusion

In this simulation of the typical perovskite solar cell, we found that by tuning active layer thickness, the device performance changes. Maximum power conversion efficiency of 22.179%is found at the perovskite thickness of 3 micron. Further, we can enhance the efficiency of the device by tuning the intermediate layer thickness and due to the addition of the dopants atom, we can enhance the stability of the device which is applicable for industrialization.

A hybrid organic-inorganic perovskite in a diode structure can lead to multifunctional device phenomena exhibiting both a high-power conversion efficiency (PCE) and strong electroluminescence efficiency (ELE). Nonradiative losses in such devices lead to an open circuit voltage (V_{OC}) deficit, which is a limiting factor for pushing the efficiency towards the

Shockley-Queisser limit. With a certain increase in perovskite thickness, PCE improves but EL efficiency is compromised and vise-versa. Thus correlating these two figures of merit of a solar cell guides the light management strategy together with minimizing nonradiative losses.

References

1. D. M. Chapin, C. S. Fuller, and G. L. Pearson, A new silicon p-n junction photocell for converting solar radiation into electrical power, *Journal of Applied Physics*, 25-5 (1954), 676-677.
2. M. A. Green, K. Emery, Y. Hishikawa, W. Warta, and E. D. Dunlop, Solar cell efficiency tables (version 41), *Progress in Photovoltaics*, 21-1 (2013), 1–11.
3. B. Parida, S. Iniyan, and R. Goic, A review of solar photovoltaic technologies, *Renewable & Sustainable Energy Reviews*, 15-3 (2011), 1625-1636.
4. H. J. Snaith, Perovskites: the emergence of a new era for low-cost, high-efficiency solar cells, *The Journal of Physical Chemistry Letters*, 4-21 (2013), 3623-3630.
5. A. Kojima, K. Teshima, T. Miyasaka, Novel Photoelectrochemical cell with mesoscopic electrodes sensitized by lead-halide compounds (2), *Meeting Abstracts: The Electrochemical Society*, (2006), 397.
6. H.-S. Kim, C.-R. Lee, J.-H. Im, Lead iodide perovskite sensitized all-solid-state submicron thin film mesoscopic solar cell with efficiency exceeding 9%, *Scientific Reports*, 2 (2012), article 591.
7. X. Li, D. Bi, C. Yi, A vacuum flash-assisted solution process for high-efficiency large-area perovskite solar cells, *Science*, 353- 6294 (2016), 58-62.
8. Z. Chen, H. Li, Y. Tang, X. Huang, D. Ho, and C.-S. Lee, Erratum: Shape-controlled synthesis of organolead halide perovskite nanocrystals and their tunable optical absorption ((2014) Materials Research Express 1 (015034)), *Materials Research Express*, 1-3 (2014), Article ID 039501.
9. T. Baikie, Y. Fang, J. M. Kadro, Synthesis and crystal chemistry of the hybrid perovskite $(CH_3NH_3)PbI_3$ for solid-state sensitised solar cell applications, *Journal of Materials Chemistry A*, 1-18 (2013), 5628-5641.
10. S. P. Singh and P. Nagarjuna, Organometal halide perovskites as useful materials in sensitized solar cells, *Dalton Transactions*, 43-14 (2014), 5247-5251.
11. M. Luan, J. Song, X. Wei, F. Chen, and J. Liu, Controllable growth of bulk cubic-phase CH3NH3PbI3 single crystal with exciting room-temperature stability, *CrystEngComm*, 18-28 (2016), 5257-5261.

12. I. Chung, B. Lee, J. He, R. P. H. Chang, and M. G. Kanatzidis, All-solid-state dye-sensitized solar cells with high efficiency, *Nature*, 485-7399 (2012), 486-489.
13. J. Burschka, N. Pellet, S. Moon, Sequential deposition as a route to high-performance perovskite-sensitized solar cells, *Nature*, 499-7458 (2013), 316-319.
14. M. M. Lee, J. Teuscher, T. Miyasaka, T. N. Murakami, and H. J. Snaith, Efficient hybrid solar cells based on meso-superstructured organometal halide perovskites, *Science*, 338-6107 (2012), 643-647.
15. J. M. Ball, M. M. Lee, A. Hey, and H. J. Snaith, Low-temperature processed meso-superstructured to thin-film perovskite solar cells, *Energy & Environmental Science*, 6-6 (2013), 1739-1743.